JOURNAL OF AIRCRAFT
Vol. 36, No. 5, September–October 1999

Full Validation of the Structural–Acoustic Response of a Simple Enclosure

S. De Rosa,* F. Franco,† F. Marulo,‡ F. Conicella,§ and G. Esposito§
University of Naples "Federico II", Via Claudio 21, 80125, Naples, Italy

This paper is a review of the basic methodologies for the study of the vibroacoustic problem of enclosed cavities. The assessment of these methodologies is addressed from the theoretical, numerical, and experimental point of view. A simple geometry has been selected as an intersection item for all three approaches, particularly for the theoretical solution. Complex geometries increase the difficulties of solving the relative equations without adding an increased value to the validity of the comparison of the three approaches. The results validate the classical finite element and the experimental approach for the vibroacoustic behavior of enclosed cavities with one elastic wall in the low modal density frequency region. As expected, a careful understanding of the numerical and experimental results turns out to be a very important task and an addressable topic for future investigations. This paper also outlines a useful comment about the aliasing effect of the wavelength discrete representation.

Nomenclature

A = length of the acoustic volume ≡ length of the plate along x direction
A_C = coupling area
B = length of the acoustic volume ≡ length of the plate along y direction
C = length of the acoustic volume along z direction
c_0 = acoustic speed of sound in an ideal gas
D = flexural plate stiffness
E = Young's modulus
F_0 = force amplitude, $F(t) = F_0 e^{-j\omega t}$
j = imaginary unit
O_{xyz} = Cartesian reference system with origin in O and axes x, y, and z, respectively
$O'_{xyz'}$ = Cartesian reference system with origin in O' and axes x, y, and z', respectively
p = acoustic pressure
t = time
w = normal plate displacement
x_F = coordinate of the point of the plate mechanically excited by the force
y_F = coordinate of the point of the plate mechanically excited by the force
∂ = derivative operator
η = structural damping
ν = Poisson's modulus
ρ = radius of the eigensolution in the plane of the mode numbers (see Fig. 3)
ρ_S = density of structure
ρ_0 = density of fluid
ω = radian frequency
∇ = gradient operator

Received 20 May 1998; revision received 20 December 1998; accepted for publication 28 December 1998.

*Senior Researcher, Department of Aeronautical Engineering, Engineering Faculty.
†Researcher, Department of Aeronautical Engineering, Engineering Faculty. Member AIAA.
‡Associate Professor, Department of Aeronautical Engineering, Engineering Faculty. Senior Member AIAA.
§Graduate Student, Department of Aeronautical Engineering, Engineering Faculty.

Introduction

THE analysis, prediction, and control of vibration and structural noise in transportation systems (trains, ships, cars, etc.) has been getting increasing attention, particularly for the design of new aircraft.[1,2] The predictive and control capabilities are needed for both low- and high-frequency ranges.[2] To increase the level of understanding for such engineering problems and to achieve reliable vibroacoustic prediction, it is important to develop both numerical and experimental tests. In a previous paper,[3] the capability of using numerical simulations such as the finite element method (FEM) and the statistical energy analysis (SEA) has been addressed without reference to an experimental support. It showed that numerical tools can give qualitatively acceptable results. However, experimental verifications are necessary to improve the reliability of FEM vibroacoustic prediction, as well as the SEA confidence intervals.

For the predictive vibroacoustic response, the FEM is now a common adopted technique,[4–6] as well as the boundary element method (BEM), whenever the coupling effect of the fluid over the structure can be neglected. Even though the vibroacoustic approach using FEM may be dated to about 15 years ago, a full-validation problem, covering results coming from the three approaches, does not always seem to have been addressed. On the other hand, SEA is the object of fundamental research and development for the high-frequency range problems, together with a tentative link with the deterministic methodologies,[7] such as the FEM (and the BEM).

In the present paper, a simple rectangular enclosure has been analyzed analytically, numerically via a FEM simulation, and experimentally. To compare the results coming from all of these approaches, a very simple design of the test article has been selected. The linear dimensions are adequate for locating a limited number of microphone acquisition points, and at the same time the enclosure can be easily removed and transported for teaching activities. The vibroacoustic behavior has been achieved by replacing a rigid wall with an elastic one. Several papers are available in the open literature regarding these aspects singularly considered, addressing generally the theory and the numerical approach, or presenting some comparisons between experimental, and again, numerical results. The present attempt is related to the possibility to develop both an analytical and numerical evaluation and laboratory tests. Several problems will be fundamentally highlighted: 1) the possibility of writing of an adequate exact solution, 2) the assembling of a correct numerical finite element model in which the user may check the validity of the wavelength simulation for both domains (acoustic and structural), and 3) the laboratory measurement campaign.

The methodologies used herein are well known and are somewhat straightforward. This should provide even more reliability to a

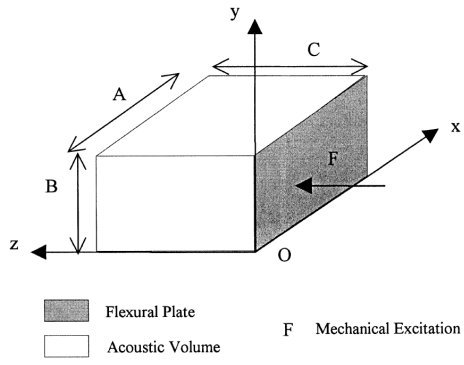

Fig. 1 Test article (real configuration).

full-validation problem. Whenever possible, this paper stresses the need for a combined approach when dealing with fluid–structure interaction problems.

Simple Enclosure

The object of study of the present vibroacoustic analysis is a regular rectangular box, whose dimensions are length 0.50 m, width 0.40 m, and depth 0.30 m. The walls were assembled by using 0.018-m-thick multilayered wood, with a thickness of 0.018 m, with a thin aluminium internal trim. The removable cover plate was replaced with an elastic steel plate (length 0.5 m, width 0.4 m, and thickness 1.0 mm). A rubber strip mounted between the sidewalls and the top cover of the box provided acoustic insulation. The boundary conditions for the cover plate were built to be considered as close as possible as simply supported along the four edges. The analytical and numerical solutions were modeled with five rigid walls; the sixth wall was elastic and was loaded by a mechanical force. A sketch of the enclosure is shown in Fig. 1. The validity of the hypothesis of rigid walls will be discussed later.

Analytical Models

The first part of the work was devoted to the analysis of assembling an analytical model of the coupled problem. Initially, both the isolated acoustic volume and plate bending equations were reviewed; these equations are coupled with the proper boundary conditions.

Uncoupled Problems

The governing equation of motion for the uniform thin plate[8] is

$$D\nabla^4 w + \rho_S h\frac{\partial^2 w}{\partial t^2} = 0 \tag{1}$$

where D is given by $D = Eh^3/12(1-\nu^2)$, and the middle plane of the plate is assumed in the x–y plane of the Cartesian reference system, O_{xyz}. It is assumed that the material is elastic, homogeneous, and isotropic. The classical simply supported boundary conditions are used along all edges of the plate. The complete modal solution of the differential equation, assuming harmonic vibrations $w(x, y, t) = W(x, y)e^{j\omega t}$, is

$$W(x, y) = \sum_{i=1}^{n}\sum_{j=1}^{M} W_{ij}\sin\left(\frac{i\pi x}{A}\right)\sin\left(\frac{j\pi y}{B}\right) \tag{2}$$

with the natural radian frequencies given by

$$\omega_{S,ij} = \sqrt{(D/\rho_S h)}[(i\pi/A)^2 + (j\pi/B)^2] \tag{3}$$

The maximum values of the coefficients N and M will be chosen as functions of the maximum frequency (minimum wavelength) to be represented.

For an ideal fluid, the acoustic pressure field is described by the Helmholtz (wave) equation

$$\nabla^2 p = \frac{1}{c_0^2}\frac{\partial^2 p}{\partial t^2} \tag{4}$$

In a general case, several boundary conditions over each face of the acoustic box can be considered:

$$p = 0, \quad \text{open wall} \quad (v \neq 0) \tag{5}$$

$$\frac{\partial p}{\partial n} = 0, \quad \text{rigid wall} \quad (v = 0) \tag{6}$$

$$\frac{\partial p}{\partial n} = -\rho_0\frac{\partial v}{\partial t}, \quad \text{elastic wall} \tag{7}$$

where v is the elastic velocity along the direction normal to the wall (the normal is positive if exiting from the fluid toward the structure).

The general modal solution for an enclosure with six rigid walls, $p(x, y, z, t) = e^{j\omega t}P(x, y, z)$, is

$$P(x, y, z) = \sum_{i=1}^{Q}\sum_{j=1}^{R}\sum_{k=1}^{S} P_{ijk}\cos\left(\frac{i\pi x}{A}\right)\cos\left(\frac{j\pi y}{B}\right)\cos\left(\frac{k\pi z}{C}\right) \tag{8}$$

Again, the maximum values of the coefficients Q, R, and S will be chosen as functions of the maximum frequency (minimum wavelength) to be represented. It is also useful here to report the general modal solution related to an acoustic enclosure with six open walls:

$$P(x, y, z) = \sum_{i=1}^{Q}\sum_{j=1}^{R}\sum_{k=1}^{S} P_{ijk}\sin\left(\frac{i\pi x}{A}\right)\sin\left(\frac{j\pi y}{B}\right)\sin\left(\frac{k\pi z}{C}\right) \tag{9}$$

The acoustic natural frequencies (eigenvalues) of both homogeneous problems [Eqs. (8) and (9)] are given by

$$\omega_{f,ijk}^2 = c_0^2[(i\pi/A)^2 + (j\pi/B)^2 + (k\pi/C)^2] \tag{10}$$

The specification of the excitation, and in general, of the initial conditions, will allow a closed-form solution to be written. A modal wave propagation along a fixed direction with symmetrical rigid-wall boundary conditions is related to the same natural frequencies of the same problem with symmetrical open-wall boundary conditions. This consideration will be clarified in the next paragraph, where this property will be used for assembling the coupled solution.

Coupled Problem

It is difficult to obtain the modal solution of coupled problems, but for the specific configuration, an efficient and formally elegant development has been introduced. The approach can be considered as a generalization of an approach presented in the open literature,[9] concerning an acoustic cubic box between square elastic plates.

For the model enclosure of dimensions A, B, and C, the following coupled structural-acoustic differential problem must be solved, in the O_{xyz} reference system indicated in Fig. 1:

Differential equations:

$$\nabla^2 p = \frac{1}{c_0^2}\frac{\partial^2 p}{\partial t^2}$$

$$D\nabla^4 w + \rho_S h\frac{\partial^2 w}{\partial t^2} = pA_C + F(t)\delta(x - x_F)\delta(y - y_F) \tag{11}$$

Boundary conditions along the four sides of the plate:

$$w = 0, \qquad \frac{\partial^2 w}{\partial x^2} = \frac{\partial^2 w}{\partial y^2} = 0 \tag{12}$$

Boundary conditions for the volume:

$$\frac{\partial p}{\partial n} = 0\ (v = 0), \quad \text{over the five (rigid) walls} \tag{13a}$$

$$\frac{\partial p}{\partial n} = -\rho_0\frac{\partial v}{\partial t}, \quad \text{over the elastic wall} \tag{13b}$$

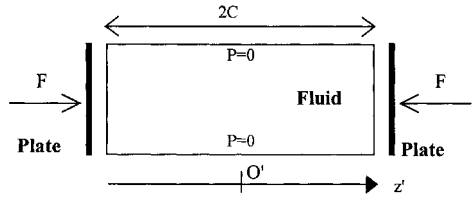

Fig. 2 Sketch of the theoretical configuration used for the analytical coupled modal solution.

The Dirac function δ has been introduced for simulating analytically the mechanical point excitation. It should be noted that the coupling conditions are in both the differential equation of the plate and the boundary conditions for the volume. For a general problem, i.e., without any symmetry and with different boundary conditions, the previous differential problem is difficult to solve. It is possible to recast the whole problem in a symmetrical form, according to the following hypothesis:

1) The effect of the fluid over the structure could be neglected; the term pA_C, the right side of the plate operator Eq. (11), will disappear in Eq. (14).

2) The length of the acoustic volume along the z direction is doubled, i.e., the length is equal to $2C$.

3) The enclosure has two elastic walls, both excited mechanically.

4) All of the other sides are open walls.

The relevance and the applicability of the first hypothesis will be discussed later. The remaining hypotheses allow the creation of a completely symmetrical model that is useful for a coupled modal representation. In the new $O'_{xyz'}$ reference system, as indicated in Fig. 2, the new differential model is the following:

$$D\nabla^4 w + \rho_S h\frac{\partial^2 w}{\partial t^2} = F_0 e^{-j\omega t}\delta(x - x_F)\delta(y - y_F),$$

$$\text{Plate 1 located at } z' = -C \tag{14a}$$

$$\nabla^2 p = \frac{1}{c_0^2}\frac{\partial^2 p}{\partial t^2} \tag{14b}$$

$$D\nabla^4 w + \rho_S h\frac{\partial^2 w}{\partial t^2} = F_0 e^{-j\omega t}\delta(x - x_F)\delta(y - y_F),$$

$$\text{Plate 2 located at } z' = +C \tag{14c}$$

Boundary conditions along the four sides of each plate:

$$w = 0, \qquad \frac{\partial^2 w}{\partial x^2} = \frac{\partial^2 w}{\partial y^2} = 0 \tag{15}$$

Boundary conditions for the volume:

$$p = 0, \quad \text{over four side (open) walls} \tag{16a}$$

$$\frac{\partial p}{\partial n} = -\rho_0\frac{\partial v}{\partial t}, \quad \text{over the elastic wall at } z' = -C \tag{16b}$$

$$\frac{\partial p}{\partial n} = \rho_0\frac{\partial v}{\partial t}, \quad \text{over the elastic wall at } z' = +C \tag{16c}$$

Figure 2 shows this new configuration. Notice the different signs in the second and third terms of Eq. (16): the normal vectors at $z' = C$ and $z' = -C$ have opposite directions.

For $z' > 0$, the problem governed by Eqs. (11–13) and Eqs. (14–16) are completely equivalent. For the sake of brevity, the first [Eqs. (11–13)] will be defined as "real," and the second [Eqs. (14–16)] as "symmetrical."

The symmetrical system contains the natural frequencies of the real problem: it has the eigensolutions with a null pressure gradient at $z' = 0$.

In the symmetrical system, the acoustic mode shapes along the y and x directions are sine functions (instead of cosine): for the determination of the pressure amplitudes inside the volume, they imply only a $\pi/2$ shift of the phases. Therefore, the symmetrical system will be able to reproduce the distribution of the vibrations and the pressure amplitudes in the real one, whereas the phase relationships are not preserved. The complete modal solution of the symmetrical problem is reported here without any further comment. It refers to a point mechanical excitation for both plates with complex stiffness, adopting the hysteretical damping model:

$$p(x, y, z')e^{-j\omega t} \Rightarrow P(x, y, z)'$$

$$= \sum_{n=1}^{Q}\sum_{m=1}^{R}\sum_{k=1}^{S} P_{n,m,k}\sin\left(\frac{n\pi x}{A}\right)\sin\left(\frac{m\pi y}{B}\right)\cos(\alpha_{n,m}z') \tag{17}$$

$$w(x, y)e^{-j\omega t} \Rightarrow W(x, y)$$

$$= \sum_{n=1}^{Q}\sum_{m=1}^{R} W_{n,m}\sin\left(\frac{n\pi x}{A}\right)\sin\left(\frac{m\pi y}{B}\right) \tag{18}$$

$$W_{n,m} = \frac{4F_0}{ABh\rho_S}\frac{\sin(n\pi x_F/A)\sin(m\pi y_F/B)}{\omega_{n,m}^2 - \omega^2 + j\eta\omega_{n,m}^2} \tag{19}$$

$$P_{n,m,k} = \frac{4F_0\omega^2}{ABh}\frac{\rho_0}{\rho_S}\frac{1}{\alpha_{n,m}\sin(C\alpha_{n,m})}\frac{\sin(n\pi x_F/A)\sin(m\pi y_F/B)}{\omega_{n,m}^2 - \omega^2 + j\eta\omega_{n,m}^2} \tag{20}$$

$$\alpha_{n,m} = k\pi/2C$$

$$\alpha_{n,m} = \sqrt{\left(\omega_{f,nmk}^2/c_0^2\right) - \pi^2(m^2/A^2) - \pi^2(n^2/B^2)} \tag{21}$$

Note that the structural natural radian frequency $\omega_{n,m}$ is unaltered due to the hypothesis of neglecting the effect of the fluid over the structure. Because of the complete symmetry of the proposed coupled model, there is no difference in the plate responses. The W function will represent the elastic displacement for both plates. Again, it must be stressed that the formulation and solution for the coupled symmetrical problem [Eqs. (11–13)] are exactly the same for the real problem [Eqs. (14–16)].

Effect of the Fluid over the Structure

As previously stated, the effect of the fluid over the plate has been neglected in the symmetrical problem. This is because the real tested configuration concerns an air-aluminium coupling, and this hypothesis can be adopted. The amount and effect of the coupling over the structural domain can be checked without approximations with the theoretical formulation of Pan and Bies.[10] This effect can be initially quantified by adopting the static ratio of the bulk modulus:

$$\lambda = \rho_S c^2/\rho_0 c_0^2 \tag{22}$$

where c is a characteristic wave speed in the structural domain. For $\lambda \gg 1$ the effect of the fluid over the structure can be neglected. By considering, e.g., the longitudinal wave speed in aluminium and fluid as air, $\lambda\ \mathcal{O}(60 \times 10^5)$, but if the fluid was water, $\lambda = \mathcal{O}(60)$.

A more precise evaluation requires a deeper analysis of the problem. Using the coupling coefficients,

$$\Xi_{vz} \propto \frac{1}{1 + \left[(\omega_{A,z} - \omega_{S,v})^2/4\right]\left(1/\Gamma_{vz}^2\right)} \tag{23}$$

with

$$\Gamma_{vz} = \int_{A_C} \Phi_{A,z}\Phi_{S,v}\,\mathrm{d}S$$

These coefficients, Ξ and Γ, refer to a generic coupling of modes: the vth structural and the zth acoustic. The Ξ coefficients are normalized and nondimensional: the closer they are to unit value, the stronger is the effect of coupling. The Γ coefficients refer only to the geometrical effect due to the coupling: the similarity of the structural and acoustic mode shapes over the coupling surface A_C for the present applications. The Ξ coefficients take into account the

dynamic effect based on the difference between the uncoupled natural frequencies. For the symmetrical configuration, the effect of the fluid over the structure is important only for the first uncoupled structural natural frequencies. However, such detailed results are outside the main topic of the present work. These considerations will be very useful when commenting on the numerical and experimental results. For an easy reading of the coupling phenomenon, a simple analytical model of a spring-mass-damper mechanical system (piston) coupled with an acoustic one-dimensional domain (pipe) has been used.[11] The undamped structural resonance was designed to be equal to the first structural resonance of the plate. Correspondingly, the acoustic natural frequencies of the pipe are the same as the longitudinal natural acoustic frequencies of the volume (along the z direction, for the sake of clarity). This simplified model has been chosen because in this case it was verified that the geometrical effect is relevant only when considering the first natural frequency of the plate and the fourth natural frequency of the acoustic cavity. This latter frequency is the acoustic mode indexed by 0, 0, 1 along the x, y, and z directions, respectively. The one-dimensional piston–pipe model includes such geometrical effects and allows the numerical measurement of the dynamic effect. The effect of the coupling is as follows:

plate:	$f_S \approx 36$ Hz	$\xrightarrow[\text{coupling}]{}$	$f_C \approx 44$ Hz
acoustic volume:	$f_A \approx 570$ Hz	$\rightarrow$	$f_C \approx 572$ Hz

The piston–pipe model only defines a modification of the structural natural frequency due to coupling. Only experimental verifications allow the measurement of this frequency shift. Moreover, it is not easy to predict a priori whether the structural frequency decreases or increases. In this particular case, it is useful to anticipate that in the experiments, the natural frequency of the structural plate is different by 8 Hz due to the coupling with the acoustic volume.

Numerical Model

The finite element approach, as implemented in MSC/NASTRAN, was used for the numerical vibroacoustic calculations. This software allows the user to select between these options:

1) Alter the standard solution sequences for simulating the fluid part of the solution and the consecutive coupling phase.

2) Use directly the standard vibroacoustic modules for the coupled solution: the coupling surface can be meshed in a 1:1 ratio (each structural node finds exactly an acoustic node that has the same coordinates), and the coupling surface can be meshed in a different ratio; an internal algorithm will find the correspondence for building the coupling nodal area matrix.

For the structural model, it was assumed to simulate the flexural wave propagation up to a maximum frequency of 500 Hz, resulting in 395 grid points corresponding to 7121 degrees of freedom. The acoustic and structural grid points are coincident over the coupling surface A_C. The acoustic model has 4752 degrees of freedom: the maximum design frequency is about 1200 Hz. Particular attention was devoted to the uncoupled and coupled modal analysis and the frequency response. The quality of output is represented by the magnitudes of the structural velocity and the acoustic pressures for some test points over the plate and inside the acoustic volume. The excitation was a 1-N white-noise spectrum mechanical force, close to the center of the panel.

Dimensioning of the Mesh

One of the more interesting results of the present work was an increasing confidence about the dimensioning procedure to be adopted for meshing a dynamic system using the FEM. It should be noted that the analyses presented here could be extended for a general deterministic methodology, or for estimating how many points are experimentally necessary to identify one requested wave. The definition of the proper mesh along one dimension at the time of a finite element model able to simulate a wave, which propagates with a characteristic speed c, comes from the following consideration. Because a minimum of five points is necessary for good identification

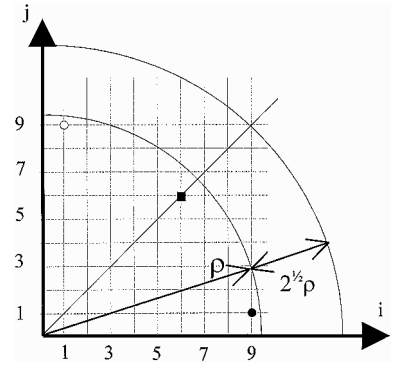

Fig. 3 Plane of the mode numbers for a rectangular aluminium plate.

of a propagating wave, the minimum number of grid points N for modeling waves up to a certain frequency $f_{\max}$ is $N = 1 + LJ/\lambda_{\min}$, where L is the length along a specific dimension, J is an integer greater or equal to 4, and $\lambda_{\min} = c/f_{\max}$.

This approach is very accurate for one-dimensional wave propagation. It may be useful to discuss the meshing for two-dimensional wave propagation, e.g., flexural waves in plates.

The previous approach is able to define a mesh, for a flexural plate, for which it is still possible to identify a mode shape very close to the design maximum frequency. This mode shape will have modal indexes very close to each other: it will be located along the bisectrix of the first quadrant of the plane of the wave numbers (Fig. 3). In this figure, the vector $\boldsymbol{\rho}$ is proportional to maximum frequency, and it identifies different mode shapes, all resonating at the same frequency. According to the outlined approach, it is not possible to take into account the fact that at natural frequencies, which are very close to each other, completely different natural mode shapes resonate. Generally, the modes with a low number of wavelengths will be better represented than the modes with a high number of wavelengths, although they resonate at approximately the same frequency. For the specific example of Fig. 3, the mode (6, 6) of the plate (represented by ■) will be represented with sufficient accuracy. The modes represented by • or ○ are contained inside the same frequency area spanned by ρ, and they have natural frequencies very close to that corresponding to ρ. They represent the (9, 1) and the (1, 9) modes, respectively.

It is easy to check that the outlined approach for dimensioning the mesh is not able to represent the mode shapes that are very close to the axes. This is due to the large difference of the indexes, even if they are inside the frequency region spanned by ρ. As a correction factor, it was found to be necessary to assume $f_{\max}\sqrt{2}$ as the maximum frequency for obtaining the correct spatial representation of all mode shapes resonating in $f_{\max}$. Conversely, if $f_{\max}$ has been retained, the result will be adequate up to $f_{\max}/\sqrt{2}$. The advantage of this meshing procedure is that it is simply dependent on the selected wave. In addition, Fig. 4 shows the error associated with the wavelength simulation with reference to the first 100 natural modes of a rectangular flexural plate. The error, reported as a percentage of the theoretical solution, is not simply a growing function of the indexes i and j (along the sides of the plate), as experienced in one-dimensional cases. The error is represented by two-dimensional distribution, with a different maximum for different pair of indexes, in the examined range. The same result could also be obtained by analyzing the following integral:

$$m_{i,j} = \int_0^{L_Y} \int_0^{L_X} \sin^2\left(\frac{i\pi x}{L_X}\right) \sin^2\left(\frac{j\pi y}{L_Y}\right) \mathrm{d}x\ \mathrm{d}y \qquad (24)$$

It is a measure of the generalized mass of a simply supported rectangular plate. The numerical solution of this integral by using linear approximations for each quadrant of the minimum desired wavelength would generate a periodic error. This effect is specifically for the simulation of two-dimensional (and three-dimensional) wave propagation. For the propagation of one-dimensional waves, the result is simply that above $f_{\max}$; the finite element model is not able to represent the wavelength. For two-dimensional wave simulations,

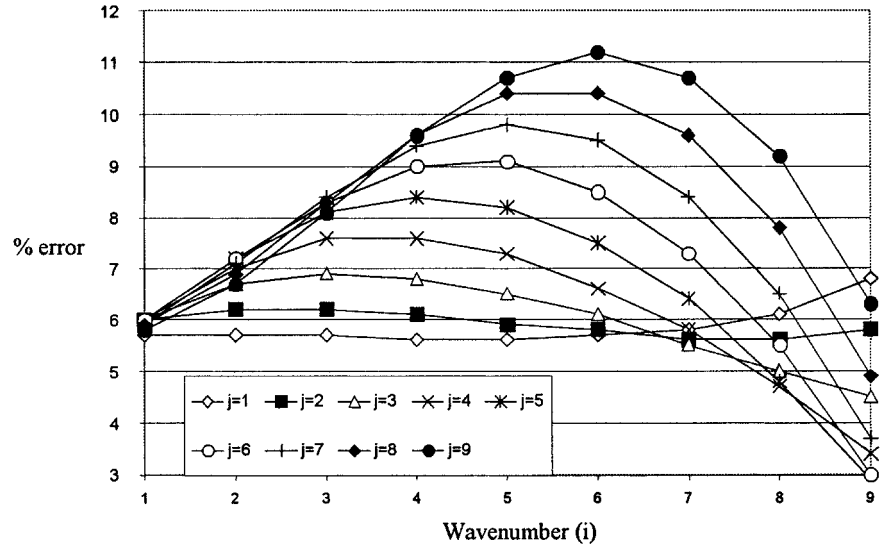

Fig. 4 Error (analytical–experimental) of the natural frequencies of a flexural rectangular plate, as a function of the half-wavelength along the edge directions.

the presented criterion of $f_{\max}\sqrt{2}$ will help in analyzing the quality of the extracted modes, and therefore, the global result of the model. It is very simple to demonstrate that, for three-dimensional wave propagation, the factor in the criterion is $f_{\max}\sqrt{3}$. Based on these criteria, the structural finite element model cannot be used for a frequency greater than ~350 Hz, and for the acoustic volume a frequency greater than 700 Hz. The results will demonstrate that the criterion is useful in determining the frequency window in which the simulations can be reliable.

Experimental Measurements

Experimental Modal Analysis of the Acoustic Enclosure

The objective of these experiments was to evaluate the natural frequencies and associated mode shapes of the acoustic enclosure; i.e., neglecting the effect of the coupling of the flexural plate. The modal measurements of the acoustic volume were carried out according to a classical procedure (Fig. 5). The selected acoustic source could be considered a point source with a wide acoustic radiation. The loudspeaker was driven by a swept sine in the time domain, for frequencies ranging from 0 to 1 kHz. The sensor microphone was a random incidence omnidirectional microphone. Aluminum plates trimmed the walls of the box to increase the reverberant capabilities of the walls, and hence, reduce the noise absorption. The acoustic enclosure was divided into 80 control volumes according to a mesh size of five grids in the x direction, six grids in the y direction, and four grids in the z direction. The loudspeaker was placed in a corner of the box. A microphone in the center of each control volume measured the acoustic signal. This methodology was used to reduce the interference effects due to the box walls in the acquisition positions closer to them. Considering that the modal density of an acoustic enclosure increases for increasing frequency, the uncertainty in evaluating the modal parameters increases with the frequency. Therefore, the proposed experimental analyses cannot exceed the 340–860 Hz frequency range, in which the first 10 natural modes are resonant. This limitation comes directly from the designed mesh size. Furthermore, the previously mentioned frequency range of the analysis has been defined by the value of the coherence function in the 0–300 and 900–1000 Hz ranges. In fact, in the 0–300 Hz range, the dynamic response of the loudspeaker is unsuitable, and in the 900–1000 Hz range, the acoustic insulation of the enclosure is poor.

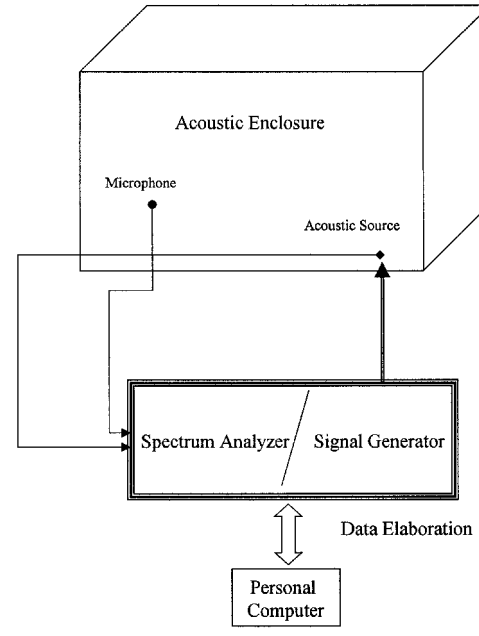

Fig. 5 Experimental setup for analysis of the acoustic volume.

Experimental Modal Analysis of the Flexural Plate

The objective of these experiments was to evaluate the natural frequencies and associated mode shapes of the flexural plate. The structural modal measurements of the plate were carried out according to a classical procedure (Fig. 6). Hammer-impact testing with a fixed

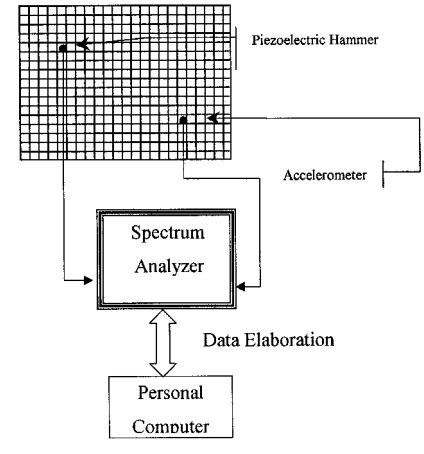

Fig. 6 Experimental setup for analysis of the elastic plate.

piezoelectric accelerometer was used for structural modal analysis. Particular care was paid to the design and manufacturing of correct boundary conditions. To obtain a simply supported condition, four aluminum beams with an L-shaped cross section (cross-sectional dimensions of 18 × 5 mm) were chosen. These beams were assembled in a knifelike position to constrain the translations while allowing the rotations on the boundaries of the plate. Nevertheless, these boundary conditions are not the ideal ones. The supports also reduce the plate dimensions and slightly limit the rotation of the plate sides. Consequently, the experimental frequencies should be higher than the numerical ones. These beams can be joined to the box, ensuring the best boundary conditions and the correct dimension of the acoustic volume in successive coupled tests. On this flexural plate a mesh size with eight grids in the x direction and seven grids in the y direction was used for the next hammer tests.

Table 1 Uncoupled structural natural frequencies, Hz

Mode	n, m	Numerical simply supported	Numerical clamped	Experimental
1	1, 1	36.5	67.2	64.3
2	1, 2	78.9	117.7	104.5
3	2, 1	103.1	154.1	124.3
4	2, 2	144.5	199.0	163.4
5	1, 3	149.9	200.2	——
6	3, 1	214.2	275.3	——
7	2, 3	213.8	287.1	——
8	1, 4	249.2	312.6	——
9	3, 2	254.2	328.6	——
10	2, 4	311.2	382.7	——

Table 2 Coupled structural natural frequencies, Hz

Mode	n, m	Numerical simply supported	Numerical clamped	Experimental
1	1, 1	44.7	70.7	60.2
2	1, 2	78.7	117.2	95.4
3	2, 1	102.9	153.6	124.2
4	2, 2	144.4	198.4	159.4
5	1, 3	150.0	200.0	168.8
6	3, 1	213.5	274.3	230.6
7	2, 3	214.3	286.6	233.1
8	1, 4	248.8	310.9	265.6
9	3, 2	253.7	326.4	272.9
10	2, 4	310.6	344.1	325.6

Forced Response

The most interesting experimental activities concern the measurement of the forced response of the flexural plate and of the acoustic enclosure in terms of acceleration and acoustic pressure level. The piezoelectric hammer provided the mechanical excitation. The impact point was selected according to the position of the excitation in the numerical and analytical analyses. The force amplitude and microphone locations were chosen to be as close as possible to the numerical and analytical models. In the following paragraphs, all results obtained during the different sessions of the experimental measurements are presented and discussed, in comparison with the analytical and numerical model.

Results

The first analysis concerns the natural frequencies of the plate. In the first phase, the elastic plate was analyzed without the effect of fluid enclosed in the volume. Table 1 compares the numerically computed and experimentally measured natural frequencies. The numerical results were carried out for two different edge boundary conditions. The results show that the numerical clamped condition of the edges is closer to the real (experimental) boundary conditions, realized by the supports, for the first natural mode. On the other hand, the experimental frequencies of higher modes are almost in the middle of the numerical natural frequencies corresponding to the two boundary conditions. These considerations confirmed that the hypothesis of a simply supported plate for the experimental analysis was not satisfied. The analysis of the coupled structural frequencies turns out to be more interesting. A comparison of results is shown in Table 2. In this case, the elastic plate encloses the acoustic volume, both in the numerical simulations and in the experiments. The effect of boundary conditions on the coupled natural frequencies is similar to the uncoupled plate response. Moreover, the natural frequencies of the plate from the second to the tenth are only slightly influenced by the fluid coupling. Only the first natural frequency is increased by a reasonable amount. To discuss this result, two types of coupling between fluid and structure must be considered, as already analyzed in the Coupled Problem section: 1) dynamic coupling (resonance conditions), if acoustic natural frequencies match structural natural frequencies; and 2) geometric coupling, if the natural modes of structural surfaces, surrounding the acoustic volume, fit acoustic modes geometrically.

In this problem, only the second condition may be analyzed, because the first natural frequency of the acoustic enclosure is approximately at 570 Hz. It is possible to demonstrate that the value of the frequency shift between the coupled and uncoupled structural natural frequencies depends on the ratio of the acoustic natural

Table 3 Analytical, numerical, and experimental natural acoustic frequencies, Hz

					Percentage difference among the methodologies		
Mode	m, n, k	A[a]	N[b]	E[c]	A–N	A–E	N–E
1	0, 1, 0	3.41E+02	3.41E+02	3.48E+02	−0.09	−2.15	−2.05
2	1, 0, 0	4.26E+02	4.26E+02	4.34E+02	−0.14	−1.83	−1.69
3	1, 1, 0	5.45E+02	5.46E+02	5.25E+02	−0.12	3.79	3.91
4	0, 0, 1	5.68E+02	5.70E+02	5.73E+02	−0.34	−0.83	−0.48
5	0, 1, 1	6.62E+02	6.64E+02	6.71E+02	−0.27	−1.31	−1.03
6	0, 2, 0	6.82E+02	6.84E+02	6.95E+02	−0.37	−1.97	−1.59
7	1, 0, 1	7.10E+02	7.12E+02	7.24E+02	−0.27	−2.04	−1.76
8	1, 1, 1	7.88E+02	7.89E+02	8.00E+02	−0.24	——-	——
9	1, 2, 0	8.04E+02	8.06E+02	8.30E+02	−0.31	——	——
10	2, 0, 0	8.52E+02	8.57E+02	8.65E+02	−0.57	——	——
11	0, 2, 1	8.87E+02	8.90E+02	——	−0.36	——	——
12	1, 1, 0	9.18E+02	9.22E+02	——	−0.50	——	——
13	1, 2, 1	9.84E+02	9.87E+02	——	−0.32	——	——
14	0, 3, 0	1.02E+03	1.02E+03	——	−0.65	——	——
15	2, 0, 1	1.02E+03	1.03E+03	——	−0.69	——	——
16	2, 1, 1	1.07E+03	1.08E+03	——	−0.46	——	——
17	2, 2, 0	1.09E+03	1.09E+03	——	−0.49	——	——
18	1, 3, 0	1.10E+03	1.11E+03	——	−0.74	——	——
19	0, 0, 2	1.13E+03	1.15E+03	——	−1.36	——	——
20	0, 3, 1	1.17E+03	1.17E+03	——	−0.72	——	——

[a]Analytical. [b]Numerical. [c]Experimental.

frequency over the structural one. Therefore, this simple analytical analysis verified that the obtained results were consistent with physical mechanisms of the fluid–structure interaction. The second phase concerns the analysis of the acoustic natural frequencies. Table 3 reports the comparison of natural frequencies of the acoustic volume, i.e., enclosed by rigid walls, for three different approaches. The agreement of these values is extremely good, particularly between the analytical and numerical frequencies.

The experimental natural frequencies of the acoustic enclosure matched quite well with those obtained from the numerical and theoretical rigid-wall models. This proved the validity of the rigid-wall assumption, together with the used acoustic excitation level.

As far as the acoustic natural frequencies are concerned (Table 3), the greater error between the experimental values and the analytical/numerical ones is in mode 3. This discrepancy may be related to the position of the loudspeaker: the adopted positions were not able to properly excite this mode shape. The excellent agreement of values among these three methodologies is due to the correct simulation of the boundary conditions. In fact, for the acoustic volume, the rigid condition of perimeter walls can be implemented correctly either in the numerical and analytical simulation or in the experimental tests. For the sake of completeness, Table 4 shows the history of the experimental acoustic natural frequencies of this enclosure. These values were carried out during the course of

Table 4 History of the acoustic experimental natural frequencies, Hz

Mode n, m, k	Analytical	Wood 1994/1995	Wood 1996/1997	Aluminum I 1996/1997	Aluminum II 1996/1997
0, 1, 0	3.41E+02	3.47E+02	3.49E+02	3.47E+02	3.48E+02
1, 0, 0	4.26E+02	4.28E+02	4.35E+02	4.38E+02	4.34E+02
1, 1, 0	5.45E+02	5.63E+02	5.03E+02	4.69E+02	5.25E+02
0, 0, 1	5.68E+02	5.81E+02	5.31E+02	5.70E+02	5.73E+02
0, 1, 1	6.62E+02	6.80E+02	5.71E+02	6.71E+02	6.71E+02
0, 2, 0	6.82E+02	7.02E+02	6.67E+02	7.18E+02	6.95E+02
1, 0, 1	7.10E+02	7.23E+02	6.90E+02	8.16E+02	7.24E+02
1, 1, 1	7.88E+02	7.98E+02	7.19E+02	8.75E+02	8.00E+02
1, 2, 0	8.04E+02	8.12E+02	7.94E+02	——	8.30E+02
2, 0, 0	8.52E+02	8.51E+02	8.14E+02	——	8.65E+02

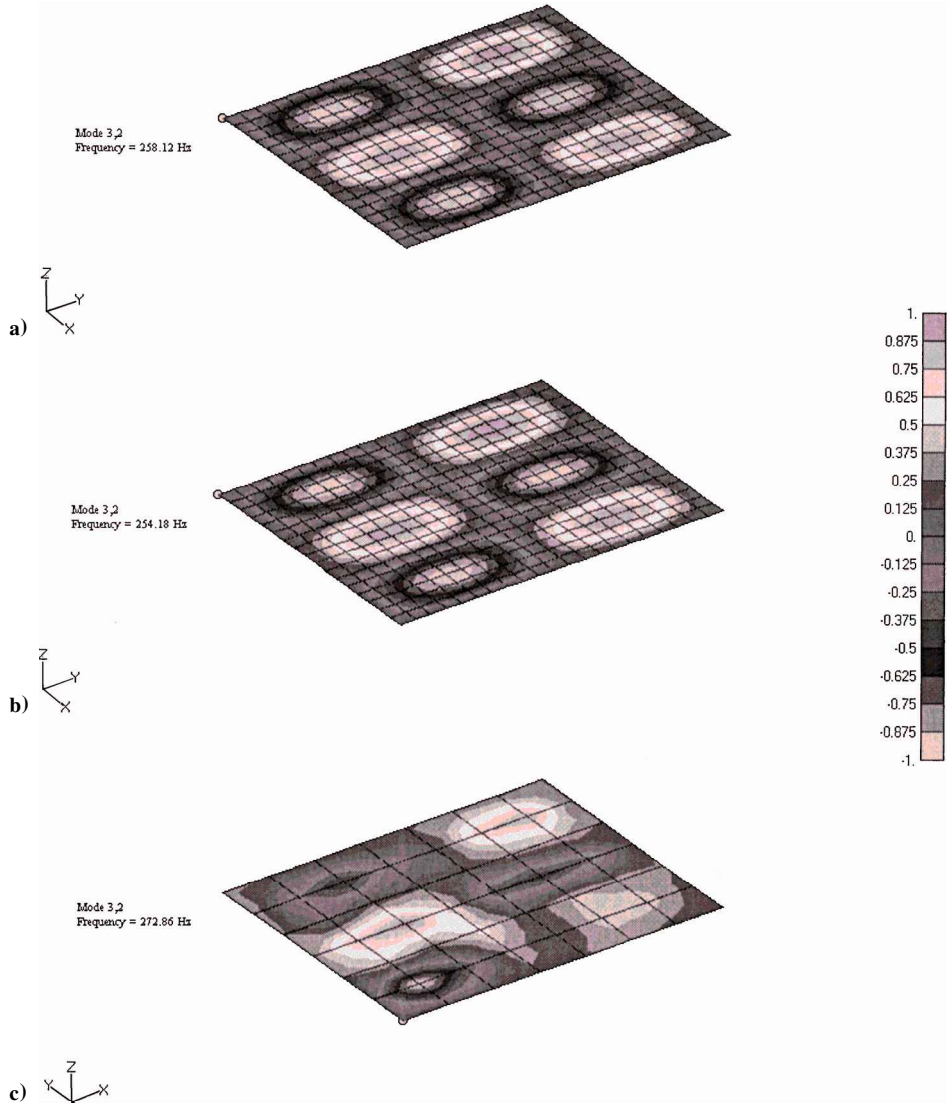

Fig. 7 Nondimensional natural mode (3, 2) of the rectangular plate (normalized displacements): a) analytical (f = 258.1 Hz), b) numerical (f = 254.2 Hz), and c) experimental (f = 272.9 Hz).

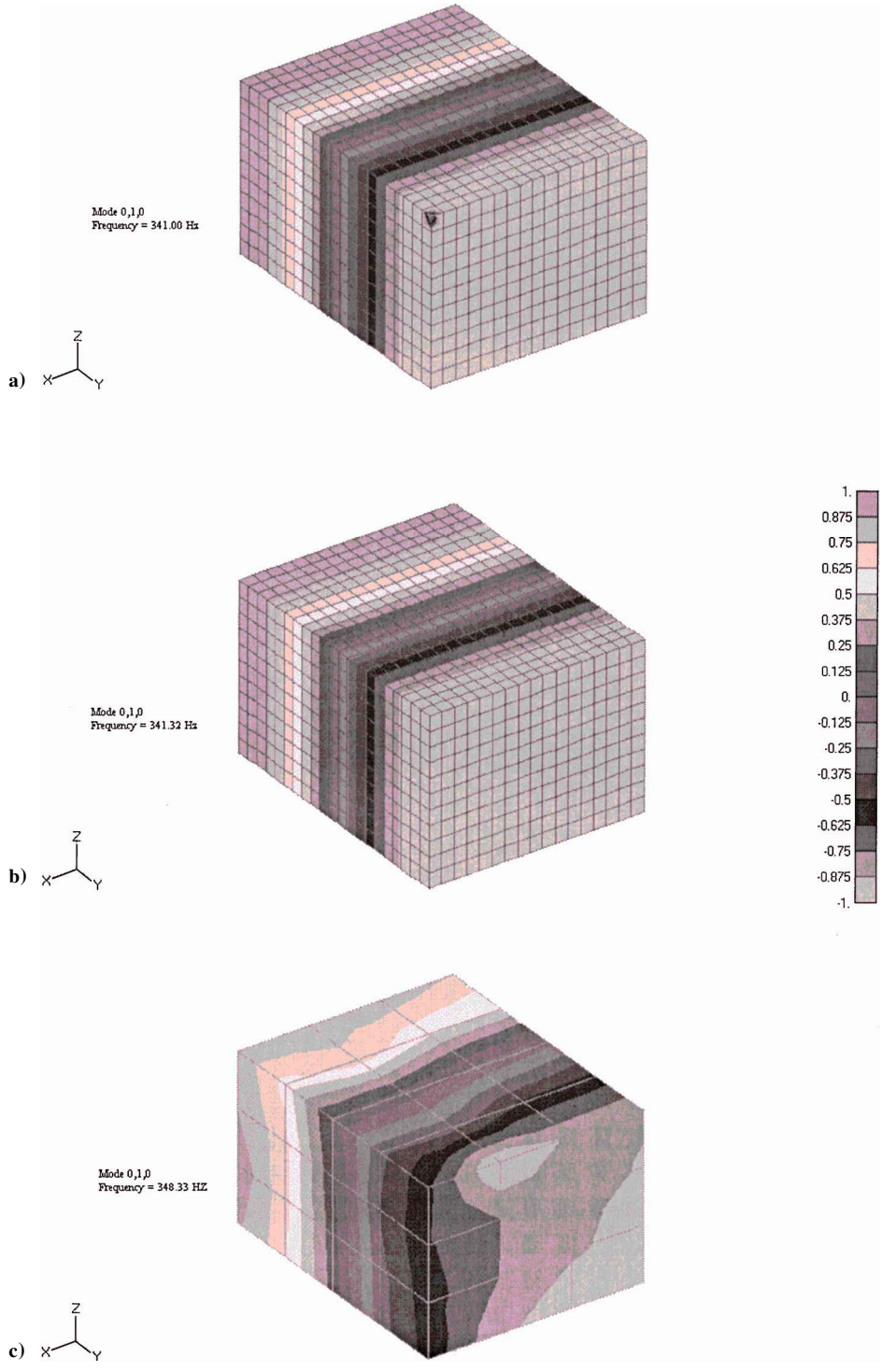

Fig. 8 Nondimensional natural mode (0, 1, 0) of the acoustic volume (normalized pressures): a) analytical (f = 341 Hz), b) numerical (f = 341.3 Hz), and c) experimental (f = 348.3 Hz).

several activities with perimeter walls trimmed by different materials. The frequency values are slightly influenced by the different conditions. In fact, because the volume dimensions remained unchanged in all tests, the differences in terms of frequencies should be related to the different wall treatments. The excellent agreement was found also in acquiring the mode shapes for both domains (Figs. 7 and 8).

A final comment concerns the analysis of the forced response of the coupled assembly (plate and acoustic volume). One must be reminded that the external excitation is produced by a hammer impact on the elastic plate. Figure 9 shows the velocity modulus vs frequency at a point on the elastic plate as obtained from the numerical model and the test. It should be noted that the numerical model was updated by using the experimental measurements. The general good agreement can be evidenced by the frequency position of the peaks and their magnitude. The same content is in Fig. 10, where the coupled response is presented. Again, a general good agreement can be evidenced by the frequency position of the peaks, but their magnitude can be correctly read only in the range of validity of the structural model, as discussed previously. It was shown that the adopted mesh for the elastic plate could not be used for a frequency greater than 350 Hz.

Similarly, the coupled model remains fully reliable for frequencies greater than 350 Hz, because in this frequency range, the model

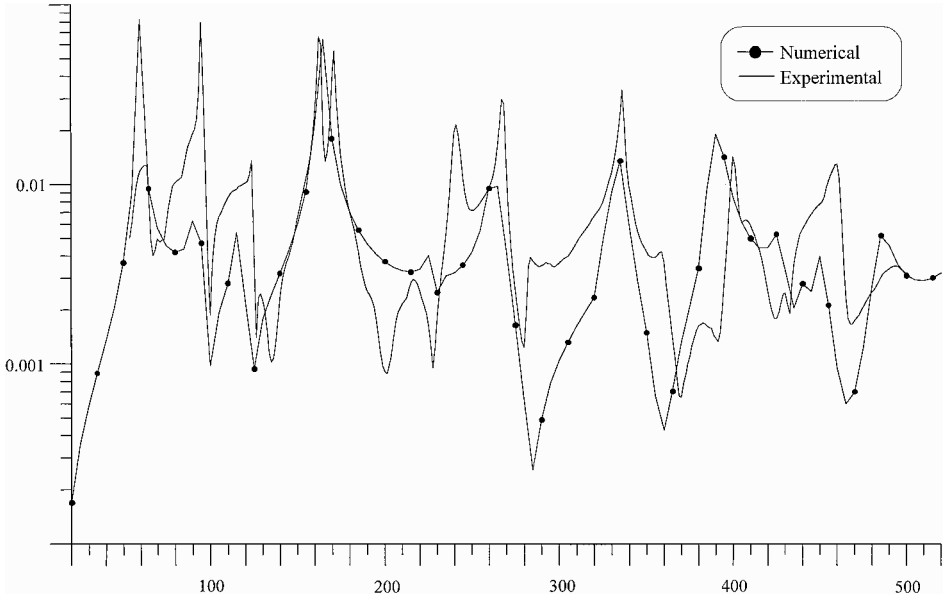

Fig. 9 Modulus of the forced velocity (m/s) for the elastic plate vs frequency (Hz), uncoupled response.

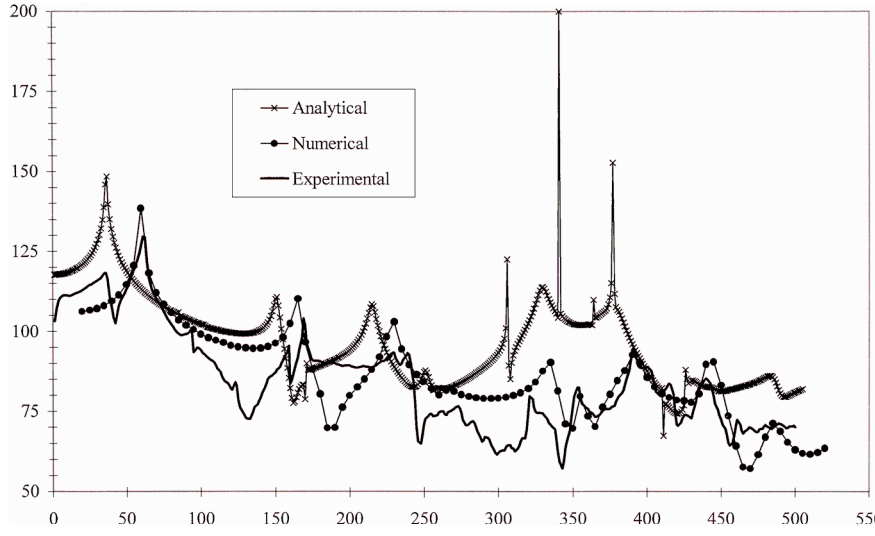

Fig. 10 Modulus of the forced pressure SPL (dB) for the acoustic volume vs frequency (Hz), coupled response.

response is completely driven by the acoustic mode shapes, which are well simulated.

The main differences evidenced in Fig. 10, between the analytical and experimental (and numerical) curves, may essentially rely on 1) the effect of the frequency shift due to a different representation of the dynamic behavior of the elastic domain because the elastic plate is simply supported along the edges in the analytical model, and 2) the absence of any damping in the acoustic part of the analytical model.

Concluding Remarks

The structural–acoustic interaction problem has been addressed with reference to a simultaneous solution of the theoretical, numerical, and experimental problems. A simple geometry, a rectangular volume with one elastic wall and the remaining five rigid walls, has been chosen as the test article. Simple considerations were drawn regarding the design of the finite element mesh able to represent the modal content up to a requested frequency range, both for the acoustic and the structural model. Strong and weak coupling cases have been outlined, evidencing that final results are not, in general, predictable as masslike (or stiffnesslike) behavior. The boundary conditions remain a critical item for the convergence of the computed results and the experimental ones, particularly for the first natural frequencies and mode shapes. The damping problem for both the structural and acoustic domains has not been addressed because it was not the specific subject of the research and because of its small effect (being a very small quantity in this case) on the results presented throughout the paper. The simplicity of the test article together with the reliability of the results may suggest a future application for studying and validating noise and vibration passive- and active-control procedures and techniques for such simple geometry.

Acknowledgments

The authors thank Centro Ricerche ed Iniziative of ANSALDO, Naples, Italy, for the support of this work. Special thanks go to A. Miele and V. Sarno for their valuable comments during the period of the collaboration.

References

[1]Landmann, A. E., Tillema, H. F., and Marshall S. E., "Evaluation of Analysis Techniques for Low Frequency Interior Noise and Vibration of Commercial Aircraft," NASA CR-181851, Oct. 1989.

[2]Mathur, G. P., and Gardner, B. K., "Interior Noise Prediction Methodology: ATDAC Theory and Validation," NASA CR-187626, April 1992.

[3]De Rosa, S., Pezzullo, G., Lecce, L., and Marulo, F., "Structural Acoustic Calculations in the Low Frequency Range," *Journal of Aircraft*, Vol. 31, No. 6, 1994, pp. 1387–1394.

[4]Wolf, J. A., and Nefske, D. J., "NASTRAN Modeling and Analysis of Rigid and Flexible Walled Acoustic Cavities," NASA TM X3278, 1975, pp. 743–745.

[5]Everstine, G. C., "Structural Analogies for Scalar Field Problems," *International Journal of Numerical Methods in Engineering*, Vol. 17, No. 3, 1981, pp. 471–476.

[6]Pezzullo, G., De Rosa, S., Bellavista, R., Sollo, A., and Cuntò, G., "A.S.C.I.A.: A General Procedure for the Structural Acoustic Calculations Using MSC/NASTRAN," *Proceedings of the 17th MSC/NASTRAN European Users' Conference*, MSC/NASTRAN Co., Los Angeles, 1992 (Paper 9).

[7]De Rosa, S., Franco, F., Ricci, F., and Marulo, F., "First Assessment of the Energy Based Similitude for the Evaluation of the Damped Structural Response," *Journal of Sound and Vibration*, Vol. 204, No. 3, 1997, pp. 540–548.

[8]Leissa, A., *Vibration of Plates*, Acoustical Society of America, Woodbury, NY, 1993.

[9]Fernholz, C. M., and Robinson, J. H., "Fully Coupled Fluid/Structure Vibration Analysis Using MSC/NASTRAN," NASA-TM-110215, Jan. 1996.

[10]Pan, J., and Bies, D. A., "The Effect of Fluid-Structural Coupling on Sound Waves in an Enclosure-Theoretical Part," *Journal of the Acoustical Society of America*, Vol. 87, No. 2, 1990, pp. 691–707.

[11]Chargin, M., and Gartmeier, O., "A Finite Element Procedure for Calculating Fluid-Structure Interaction Using MSC/NASTRAN," MSC/NASTRAN Co., Documentation Rept., Los Angeles, May 1990.